

Nitrogen-Stabilized DLC Coatings: Optimization of Properties and Deposition Parameters Using Randomized Tree and Neural Network Algorithms

A. I. Voropaev¹, V. I. Kolesnikov¹, O. V. Kudryakov^{2*}, V. N. Varavka²,
I. V. Kolesnikov¹, M. S. Lifar^{1,3}, S. A. Guda^{1,3}, A. A. Guda^{1,3}, and A. V. Sidashov¹

¹ Rostov State Transport University, Rostov-on-Don, 344038 Russia

² Don State Technical University, Rostov-on-Don, 344000 Russia

³ Southern Federal University, Rostov-on-Don, 344090 Russia

* e-mail: kudryakov@mail.ru

Received July 10, 2023; revised September 11, 2023; accepted September 25, 2023

Abstract—This work discusses the predictable control of plasma-assisted physical vapor deposition (PVD) of coatings. The multiple process parameters and the instability of the nonequilibrium ion plasma system create substantial obstacles to the wide industrial application of promising multicomponent functional coatings. Here we propose a solution to this problem, which includes: creation of a database of diamond-like carbon (DLC) coatings to identify a limited set of adjustable process control parameters, determination of how these parameters affect the coating properties, analysis of the revealed effects using statistical methods and neural network algorithms, and use of the results for the predictable tuning of specified coating properties. The object of research is original DLC coatings whose structure is stabilized with nitrogen instead of conventionally used hydrogen. The experimental database of DLC coatings is created based on our previous studies and includes structural, morphological and architectural characteristics of coatings, various types of substrates, sublayers, physical, mechanical and tribological properties, and various combinations of coating deposition parameters. A specific problem is solved to determine the influence of deposition parameters such as chamber pressure P , stabilizer content (% nitrogen), ion flux rate (coil current λ) and deposition time t on hardness H and elastic modulus E of coatings. Based on the results obtained, the deposition parameters are optimized so as to obtain predictable strength values of the formed carbon coating. The optimization procedure is developed using both classical statistical methods and modern algorithms of ridge regression, randomized trees (ExtraTrees), and a fully connected neural network (multilayer perceptron MLP).

Keywords: plasma-assisted physical vapor deposition, coating deposition parameters, DLC coatings, microstructure, scanning electron microscopy, X-ray photoelectron spectroscopy, indentation, physical and mechanical properties of coatings, database, neural network algorithms

DOI: 10.1134/S1029959924040015

1. INTRODUCTION AND PROBLEM STATEMENT

Despite a long history of plasma-assisted deposition technology, there are great difficulties with its application to industry, including tool production, microelectronics, optics, medicine, and to a very limited extent mechanical engineering, thermal power engineering (turbine blades, valves, etc. [1–7]) and decorative arts (gold-colored titanium nitride films). The main problem in technology transfer is the multi-parameter nature of the process [7, 8]. The variety of vacuum systems, vapor deposition techniques, and

apparatuses for plasma-assisted deposition leads to a very complex set of parameters, each of which determines the final composition, structure and properties of the coating. In the most general terms, the set of parameters can be divided into several groups: process parameters and substrate parameters are considered as input parameters, and coating parameters are regarded as output parameters. The first and largest group of process parameters, e.g., in arc evaporation, includes such characteristics as the number and quality of cathodes, arc current and voltage, operating chamber pressure, deposition rate, bias voltage, de-

position angle, presence or absence of magnetic separation, and others. Magnetron sputtering parameters are somewhat different, but their number is also large. As for the substrate parameters, it is necessary to account for the substrate composition, surface quality (roughness, chemical purity, the presence of stresses, etc.), structural-phase state, mechanical characteristics, temperature, and temperature drift during deposition. The group of output parameters is determined by the coating functionality, and it can also be very extensive. This group necessarily includes the elemental composition, parameters of the structural-phase state (number, dispersion and morphology of phases, structural type of coating in accordance with the Movchan–Demchishin–Thornton diagram [9, 10]), coating architecture (2D/3D morphology, single/multilayer), and a set of properties determined by the coating service conditions. As a result, the total number of descriptors needed for the programmable coating deposition can include 20–40 parameter values. In this regard, the predictable synthesis of plasma-deposited coatings is related to the use of machine learning and neural network algorithms, which cannot be tested without adequate databases. The need for the use of artificial intelligence in plasma-assisted vapor deposition of coatings has been recognized only recently due to its successful applications. One of the first databases was created specifically for diamond-like coatings (DLC) [11], which included the results of about 80 researchers published in more than 100 articles. The constantly updated database currently contains data for more than 800 coatings, including 25 types of DLC coatings (a-C:H, a-C, Cr-DLC (a-C:Cr), Ti-DLC (Ti-C:H), etc.) and 16 types of methods for their deposition. It also includes tribological coatings, grouped according to 55 types of counterbodies and 9 friction test methods. However, the search for optimal combinations of descriptors for each data set, including using the here presented database, is in a very early stage [12–14].

The accurate prediction of properties of plasma-assisted PVD coatings is also complicated by the fact that plasma is a nonequilibrium state of matter that is able to evolve from one unstable state to another under the influence of fluctuating parameters. A prediction system for such transitions has not yet been developed. That is why coatings deposited with the same technology and equipment, with the maximum number of fixed parameters, show a wide scatter of values, making the use of computer-aided prediction algorithms less effective. For example, inhomogeneities in the evaporated material lead to unstable plas-

ma discharge and therefore inhomogeneous ion flux. In this work, we use sintered graphite powder cathodes that contain pores, interparticle melting zones, and powder particles with different crystallographic orientations. During laser evaporation of graphite, all these inhomogeneities present fluctuating (random) parameters that affect ion flux during DLC coating deposition [15, 16].

Thus, predictable control of plasma-assisted coating deposition is a serious challenge in modern surface engineering. One of the ways to solve this problem is to identify universal relationships (at least empirical) between the group of variable process parameters and coating properties. This will help reduce the total number of control parameters and the influence of fluctuations in coating technology. The main purpose of this work is to create a database of reliable experimental data, to analyze the data using neural network algorithms, and to establish universal relationships for diamond-like carbon coatings.

2. MATERIALS AND METHODS

The substrates used in the study were polished plates (roughness grade not less than 10 with $R_a \leq 0.12 \mu\text{m}$ and $R_z \leq 0.6 \mu\text{m}$ according to GOST 2789-73) with dimensions of $50 \times 30 \times 5 \text{ mm}$ made of low-alloy structural steel 40CrNi2Mo with tempered sorbite structure (after hardening and high tempering at 600°C), which is widely used in mechanical engineering. This substrate material was chosen because it is often used in loaded friction units whose contact surfaces can be effectively protected by DLC coatings [17–19]. The physical and mechanical characteristics of 40CrNi2Mo steel substrates after quenching and high tempering were: $H = 2.5 \text{ GPa}$, $E = 200 \text{ GPa}$, $H/E = 0.0125$, $H^3/E^2 = 0.00039 \text{ GPa}$.

In comparison with similar physical and mechanical characteristics of diamond-like coatings, the substrate samples were soft (plastic). A significant difference in the properties could negatively affect the adhesion of coatings, so we also examined cases with DLC coatings deposited on a Ti or TiN sublayer.

Plasma-assisted deposition of carbon coatings was carried out on a BRV600 vacuum unit (BelRosVak LLC, Belarus), which includes both three-cathode arc evaporation of metallic materials and magnetron sputtering from targets of various compositions. The unit is equipped with a high-power ion source and a system for sputtering carbon coatings by laser evaporation of graphite.

Table 1. Experimental relationships between the values of the parameters %N and P_N of the BRV600 test unit

%N, %	0	1	2	3	4	5	6	7	8	9	10
P_N , Pa	0.00034	0.0056	0.013	0.021	0.031	0.041	0.053	0.066	0.078	0.092	0.11
%N, %	11	12	13	14	15	16	17	18	19	20	
P_N , Pa	0.12	0.14	0.15	0.17	0.19	0.20	0.22	0.23	0.25	0.27	

Before coating deposition, the surface of the samples was ion etched in a built-in Ar ion source at a chamber pressure of ~0.7 Pa, a temperature of ~400°C, and a bias voltage of 1000 V for 5 min. Since the system was initially multiparameter, some of the parameters should be fixed to reduce the number of experiments and ensure the reproducibility and a more accurate analysis of experimental results. As fixed coating deposition parameters for testing the operating modes of the BRV600 unit, we took the characteristics of the carbon sputtering system, which remained unchanged in all experiments:

- graphite evaporation source was Q-switching laser (without an amplifier) $Q_{sw} = 350 \mu s$,
- arrester voltage 300 V,
- laser frequency 10 Hz,
- laser radiation energy 600–700 mJ,
- cathode scanning speed (stepper motor speed) 1 mm/s,
- laser scanning was performed across the end surface of the cathode rotating about the cylinder axis with a speed of 1 rpm,
- cylindrical cathodes were made of VP-6 graphite powder.

The following were selected as variable parameters that determine the range of measured and optimized properties of the coating:

- operating chamber pressure $P = 0.011\text{--}0.31$ Pa,
- induction coil (solenoid)¹ current $\lambda = 1\text{--}5$ A,
- the amount of nitrogen supplied to the chamber %N = 1–5 (determined in % by the gas supply valve of the test unit),
- coating deposition time $t = 10\text{--}35$ min.

The parameter %N is especially noteworthy. In this work, the structure of DLC coatings was stabilized with nitrogen instead of explosive hydrogen (see below for details). Typically, the use of plasma-form-

ing gases (Ar, H₂, N₂, C₂H₂, CH₄, etc.) in vacuum technologies is characterized by the partial pressure value (P_N for nitrogen). However, in technological practice, particularly in the BRV600 unit, the working gas is supplied to the chamber through regulating valves that are calibrated in percentage of valve opening (%N for nitrogen). This process parameter is convenient in practice and in experiments (e.g., due to smooth adjustment at small %N values). Therefore, we used the parameter %N in experiments and for database creation to characterize the amount of nitrogen in the working chamber during coating deposition. The nonlinear correspondence between the parameters %N and P_N obtained on the basis of empirical data from the BRV600 unit is shown in Table 1. If necessary, it can be used to transcribe the results obtained in this work depending on the parameter P_N .

One of the drawbacks of carbon coatings is that tetrahedral amorphous carbon (ta-C) films with an over 70% sp³ bond content and a thickness exceeding ~500 nm are prone to spontaneous cracking. To increase the coating thickness, which is often required for their applied use, the coatings are stabilized with hydrogen. The most common working gases for the production of ta-C:H coatings are acetylene C₂H₂ or methane CH₄. This technology, with all its advantages, has an increased fire and explosion hazard. Here we made an attempt to stabilize DLC coatings with nitrogen, which was used as a working gas instead of explosive carbon gases. The nitrogen stabilizer content in the coating is actually controlled by the parameter %N.

In carbon coating studies, nitrogen is used as an alloying element to form, e.g., amorphous carbon nitride a-CN_x films [20, 21]. Differences in the structure of amorphous carbon with a sp³ bond content of no more than 30–50% (a-C) and amorphous carbon nitride (a-CN_x) are demonstrated in Fig. 1. In the case of a-CN_x films, nitrogen atoms change the structure of carbon films, increasing the number of phonon modes available for excitation [22]. It is believed that a-CN_x films have a fullerene-like microstructure with curved and intersecting basal planes. The instrumental determination of such a microstruc-

¹ BRV600 unit has five solenoids (induction coils): solenoids 1–3 are used for deposition of cermet coatings in the main chamber, solenoids 4, 5 are used for deposition of carbon coatings; the coil current magnitude determines the flux rate of deposited carbon ions.

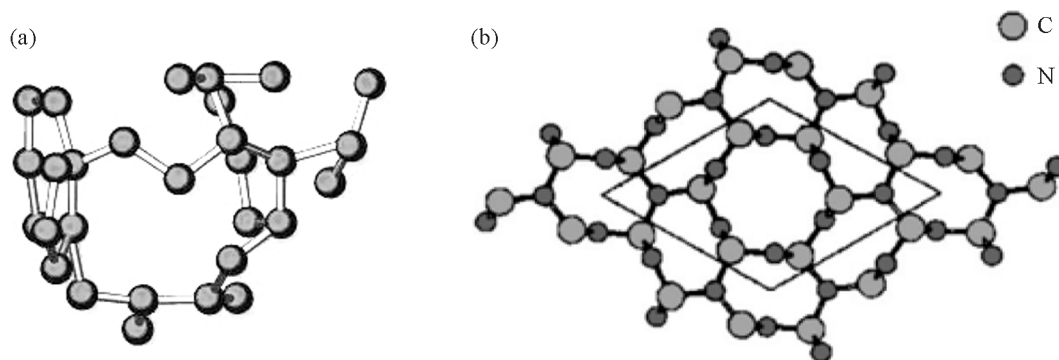


Fig. 1. Schematic view of the atomic structure of carbon a-C (a) and a-CN_x coatings (b).

ture is very problematic and can be done, perhaps, only by molecular dynamics simulations.

Most of the coating studies were carried out using scanning electron microscopy, X-ray (EDX) microanalysis, and X-ray photoelectron spectroscopy (XPS). The physical and mechanical properties of samples were evaluated by continuous indentation tests.

The microstructure, surface condition and fine structure of the coatings were examined by scanning electron microscopy on a ZEISS Crossbeam 340 dual beam microscope, which combines high-resolution electron microscopy (up to 2 nm) with the possibility of surface etching and cross-sectional sample preparation by an ion beam directly in the vacuum chamber of the microscope, which allows a deep examination of all types of surfaces at the nanostructural level. Linear assessment of layer thickness, inclusion sizes, phase components, pores, etc. was done using AZtec software for an electron microscope.

The chemical composition of the coatings was determined on an energy dispersive X-ray spectrometer (EDAX) X-Max 50N (Oxford Instruments) coupled with the ZEISS Crossbeam 340 electron microscope.

The accuracy of the data on the elemental and phase composition of the surface, thin surface layers, films and coatings was improved by experimental studies on a surface analysis system (SPECS, Germany) using X-ray photoelectron spectroscopy. The monochromatic AlK_α line with an energy of 1486.6 eV was chosen as the exciting radiation. The energy resolution of the analyzer at constant transmission energy was 0.45 eV at the Ag3d_{3/2} peak. The vacuum during spectra recording was maintained at a level of 1×10^{-10} mbar. The error in measuring the binding energy and line widths at half maximum (FWHM) was ± 0.1 eV, and in relative intensity measurements it was $\pm 10\%$.

The qualitative and quantitative composition of the surface was analyzed by XPS survey spectra. In addition, photoelectron lines were determined for the chemical elements on the surface by which it was possible to reliably identify the chemical bond where a particular element was involved. As a result, we could determine the phase to which this element belonged. The SPECS surface analysis system is equipped with an ion gun for surface sputtering and allows recording spectra at each depth. It also has a special program for decomposing experimental spectra into components, each of which corresponds to a specific chemical bond. Of great importance are the experimental statistics for plotting smooth curves and the scanning step. In most cases, spectra were obtained with a scanning step of 0.1 eV and a maximum number of pulses of up to one hundred thousand. The uncertainty in the spectral line profile in this case reached about $\sim 0.3\%$, and the relative error (intensity ratio of two lines) was no more than 2–3%. Thus, the XPS method can be used to experimentally determine, with great accuracy, changes in the element content and its chemical bonds across the thickness of a thin layer, film or coating.

The physical and mechanical properties of samples at the nano- and microscale were examined using a Nanotest 600 test platform. The elastic modulus E and hardness H were determined by continuous indentation tests [23]. Microscale measurements (load less than 2 N, indentation depth more than 0.2 μm) were conducted with a tetrahedral Vickers indenter, and a triangular Berkovich indenter was used for nanoscale measurements (indentation depth no more than 0.2 μm). The tests and processing of the obtained data were carried out in accordance with GOST 8.748-2011 [24]. The measurements were performed on 3–7 samples of the same type. Indents were made in three different randomly selected and spaced zones

on the surface of each sample, which corresponded to the positioning of the optical system of the Nano-test 600 platform. Within each zone, indents were located evenly, with the minimum possible density. The statistical processing of the measurement results was carried out taking into account at least 10 indent values in each positioning zone. The total number of indents in each zone was different and depended on the quality of the coating surface; indents made on surface defects or in high roughness areas were not taken into account in statistical data processing. This study reports the average estimates of the measured values in accordance with the data processing recommendations of GOST R 50779.25-2005 and GOST R ISO 16269-4-2017 [25, 26]. In addition to the structure-dependent hardness H and the structure-independent elastic modulus E determined by the indentation method, metallic materials are often characterized by the ratios of H/E and H^3/E^2 . The first ratio determines the resistance to elastic deformation and is often an indirect indicator of the level of, e.g., tribological properties: the higher the H/E , the higher the wear resistance during friction [27; 28, p. 608]. The H^3/E^2 ratio determines the resistance of the material to plastic deformation [29, p. 134].

Using the above research methods and by varying the deposition parameters, we created an experimental database for DLC coatings. Its fundamental differences are: (i) the use of laser evaporation of graphite instead of magnetron sputtering used in [11], (ii) the use of sublayers of various compositions, and (iii) the substrate made of a commercial material, unlike Si or corrosion-resistant austenitic steel 08Cr18Ni10Ti often used for purely research purposes. The results of the database analysis and processing are presented in subsequent sections of the paper.

3. RESULTS AND DISCUSSION

3.1. Composition and Structure of Coatings

The typical structure of the studied DLC coatings is shown in Fig. 2. The carbon coatings are single layers with a thickness of 0.6–1.4 μm . Their structure is generally characterized by high density and homogeneity. In some cases, the cross-sectional coating structure reveals hardly distinguishable layers (Figs. 2a–2c), which can probably be caused by diffusion processes at the substrate–coating and coating–medium interfaces. The reasons for the formation of the layers were not studied in more detail. The database of DLC coatings was created using various sublayers (Figs. 2d–2h). The sublayer was mainly ap-

plied for tribological purposes in order to reduce stresses at the substrate–coating interface, but the tribological aspect of the coatings was not discussed.

Electron microscopic examination revealed tight adherence of the coating to the substrate. The boundary between them does not show any defects or signs of deformation, which can be characterized as satisfactory adhesion. High-rate deposition modes led to the formation of porosity in the sublayer (Figs. 2e and 2f), especially pronounced closer to the substrate. However, as can be seen from the micrographs, the presence of porosity in the sublayer did not affect the tightness and morphology of the sublayer–substrate and sublayer–coating interfaces.

The samples in all micrographs in Fig. 2 are tilted toward the observer at an angle of 15° – 28° to demonstrate the coating surface morphology. One can see some single artifacts and droplet defects that are in the stage of healing [30], i.e., gradual smoothing of valleys due to the deposition of new atomic layers of the coating. The surface quality is in general satisfactory and does not affect the measurement results of physical, mechanical or tribological properties of coatings. A typical distribution of chemical elements in the resulting carbon coatings is presented in Fig. 3.

The physical meaning of using nitrogen in a DLC coating, whose content is controlled by the parameter %N, is to stabilize the carbon layer. The role of nitrogen is similar to that of hydrogen in DLC coatings, and it is used to replace explosive hydrogen in the considered plasma-assisted deposition technology. The use of stabilizers should not lead to the formation of new phases in the coating, but is intended to modify the spatial distribution of carbon atoms (Fig. 1). Note that electron microscopy revealed no new phases in the resulting coatings. The use of nitrogen as a stabilizer also resulted in coatings with a thickness much greater than the critical thickness of pure ta-C coatings, which is ~ 500 nm. The stress-strain state of the ta-C coating due to larger thickness leads to its spontaneous brittle cracking and chipping [31, 32].

A qualitative analysis of the coatings on each sample was carried out using the XPS method. Survey spectra were obtained, one of which is shown in Fig. 4a. The survey spectra were used to select energy ranges for scanning the 1s lines of carbon, oxygen, nitrogen and sodium, and the 2p lines of chlorine and sulfur (their presence on the surface is due to contamination during sample preparation). The kinetic energy range of 230–301 eV was chosen to record C(KVV) Auger electron spectra of carbon (Fig. 4b).

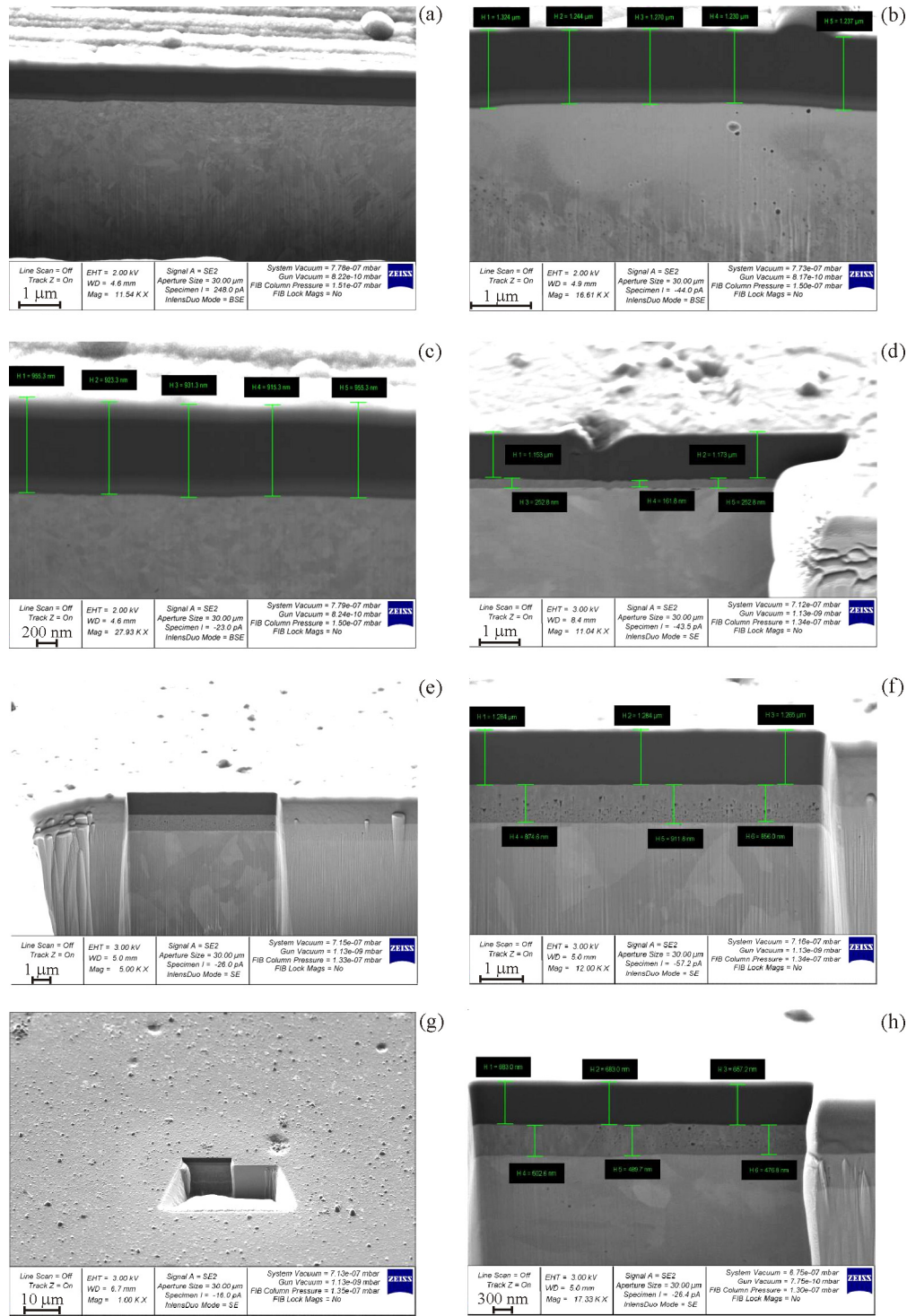


Fig. 2. Cross-sectional structure of nitrogen-stabilized DLC coatings (SEM, FIB cross-sections): a–c—carbon coatings of different thickness without a sublayer, d–f—carbon coatings with a Ti sublayer of different thickness, g, h—carbon coating with a TiN sublayer.

The spectral background during quantitative analysis for XPS spectra, caused by elastically scattered electrons, was subtracted by the Shirley method using Casa XPS SPECS software. XPS analysis data on the

surface chemical composition of the DLC-coated samples are given in Table 2.

The sp^2/sp^3 carbon content was determined from the C (KVV) Auger spectra shown in Fig. 4. Data on

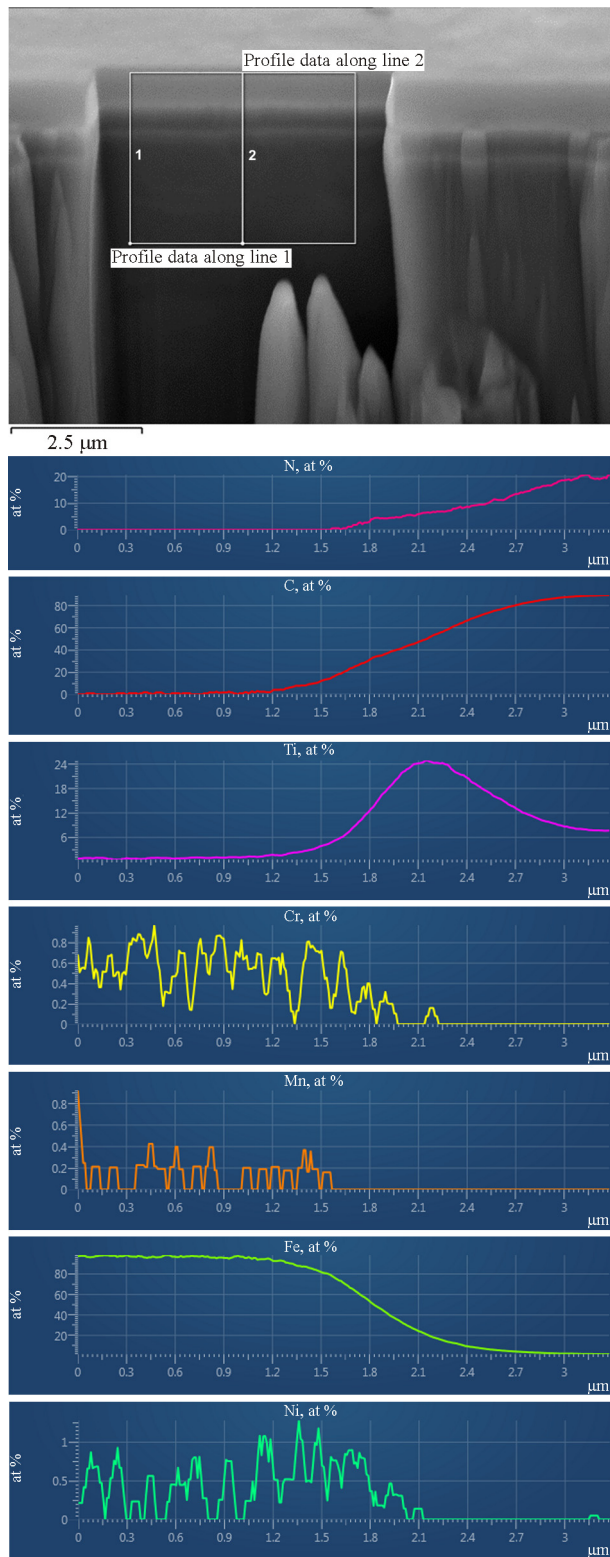


Fig. 3. Through-thickness distribution of elements in a nitrogen-stabilized DLC coating with a Ti sublayer, EDAX data—distribution along the secant line (line 2 perpendicular to the surface) from the substrate towards the surface of the DLC layer (color online).

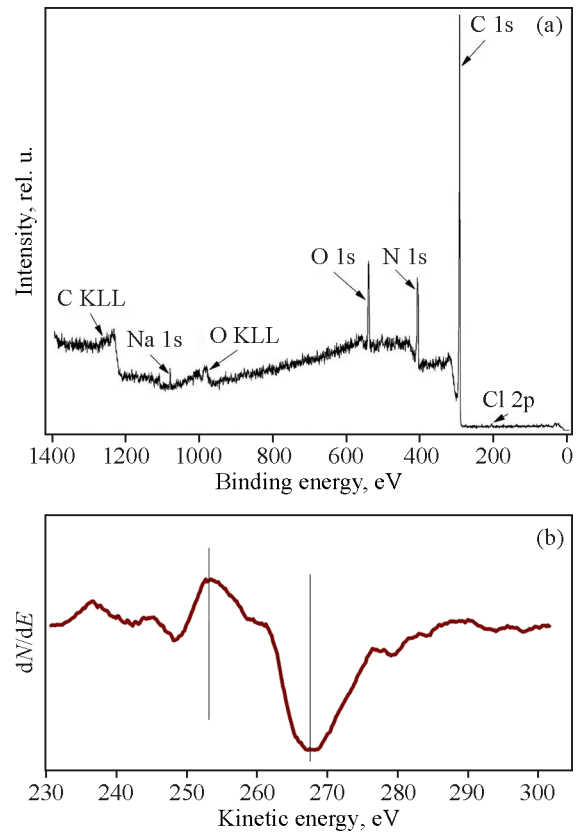


Fig. 4. XPS survey spectrum from the surface of the DLC carbon coating (a), and C (KVV) Auger spectrum for estimating the sp^2/sp^3 carbon content in the coating (b).

the sp^2 and sp^3 fractions in the synthesized films were obtained using X-ray excited C (KVV) Auger electron spectra along with XPS C1s spectra. The initial basis spectra for quantitative assessments were the C (KVV) Auger spectra of graphite with $sp^2=1$ and the spectra of diamond with $sp^2=0$, which are usually used to identify the hybridization state of carbon atoms [33–36]. The distance between the maximum and minimum in the differentiated C (KVV) spectrum, marked in Fig. 4b, corresponds to a sp^3 carbon content of about 70%. The relationship with different relative fractions of sp^2 and sp^3 phases was derived using the equation $sp^2/sp^3 = x/(1-x)$, for the x fraction of the sp^2 phase varying from 0 (diamond) to 1 (graphite) [30].

The results obtained (Table 2) show that the carbon coatings synthesized on 40CrNi2Mo steel samples can be classified in accordance with modern concepts as DLC coatings and assigned to nitrogen-doped tetrahedral amorphous carbon (ta-C:N) coatings. This is indicated by the presence of nitrogen in

Table 2. Results of XPS quantitative analysis of the chemical composition and electronic configurations of carbon coatings

Coating characteristics	Elemental composition of the coating surface, at %						Bond content, fractions	
	O 1s	C 1s	N 1s	Na 1s	Cl 2p	S 2p	sp ²	sp ³
Coating with survey spectrum (Fig. 4)	6.3	78	15	0.36	0.34		0.28	0.72
Database summary results	5.6–12.0	72.2–92.4	2.0–16.5	0.1–0.7	0.2–0.4	0.5–0.8	0.1	0.9

the coating (2.0–16.5%), which according to XPS data forms no bonds typical of chemical compounds, and by the high content of diamond-like sp³ carbon configuration exceeding 70% in all studied coatings.

3.2. Effect of Deposition Parameters on the Physical and Mechanical Properties of Coatings

The generated experimental database of DLC carbon coatings was used as the main source of information for plotting the curves of the measured physical and mechanical properties of coatings against coating deposition parameters. It was also used to implement machine learning and neural network algorithms, the results of which are presented in the following section.

The physical and mechanical characteristics considered are the elastic modulus E and hardness H determined by continuous indentation tests in accordance with measurement procedures and available equipment [23–26]. The group of physical and mechanical properties also included the calculated values of H/E and H^3/E^2 ratios, which determine the coating resistance to elastic and plastic deformation, respectively [24–26]. However, with a sufficiently large sample of data, these ratios are very similar to the dependences of the most unstable component of the ratio that is hardness H for plasma-assisted PVD coatings. Therefore, the curves of the H/E and H^3/E^2 ratios versus variable deposition parameters (P , λ , $\%N$, t , see Sect. 2) are not given, because their variation is qualitatively the same as that of the hardness curves.

As a result of statistical processing, one-parameter curves were obtained showing the effect of the coil current λ , which characterizes the volumetric flux density of deposited carbon ions, and the amount of nitrogen supplied to the chamber $\%N$ on the physical and mechanical characteristics of coatings E and N (Figs. 5 and 6). Since the variation of deposition parameters was discrete, the average statistical values of hardness H corresponding to each fixed value of the parameters λ and $\%N$ are marked with dots in Fig. 5. In addition to the curve of the statistical avera-

ges of H (Medium), Figs. 5a and 5b show the scatter ranges of H (Maximum–Minimum) observed in the database as a whole.

The resulting dependence $H=f(\%N)$ is quite complex. It can be approximated by a third-degree polynomial, but the accuracy of such an approximation is unsatisfactory: the root mean square (RMS) error is 13.26 GPa and higher (i.e., exceeds 50%). Therefore, the approximation curve for this dependence was not plotted. Nevertheless, the dependence $H=f(\%N)$ in Fig. 5a is quite indicative even without approximation. The $H=f(\%N)$ curve clearly defines the interval of optimal values for the parameter $\%N$, equal to $N=5$ –8%.

The $H=f(P)$ and $H=f(t)$ curves are not presented in this section due to their very simple geometry with a clear physical meaning. The dependence $H=f(P)$ increases almost linearly as the vacuum improves, which corresponds to the physical meaning of plasma-assisted sputtering in vacuum: the lower the pressure in the working chamber, the less the ion flux is obstructed during coating deposition. The introduction of nitrogen into the chamber disrupts the linearity of this dependence, because nitrogen stabilization of carbon coating (parameter $\%N$) has a stronger and nonlinear effect on coating hardness H (Fig. 5a). Sputtering time t has a linearly proportional effect on the coating thickness, but has virtually no effect on hardness H . The dependence $H=f(t)$ remains practically constant throughout the entire variation range of the parameter $t=10$ –35 min (subject to the correct indentation procedure during which the load should be adjusted depending on the coating thickness in accordance with [24]).

Of the hardness curves plotted, only the $H=f(\lambda)$ curve can be approximated by the least squares method (LSM) with satisfactory accuracy (Fig. 5b). The third-degree polynomial (1) describes the experimental dependence $H=f(\lambda)$ with an RMS error of 1.68 GPa (Fig. 5c):

$$H(\lambda) := 24.3235 - 17.3861\lambda + 8.29617\lambda^2 - 0.9285882\lambda^3. \quad (1)$$

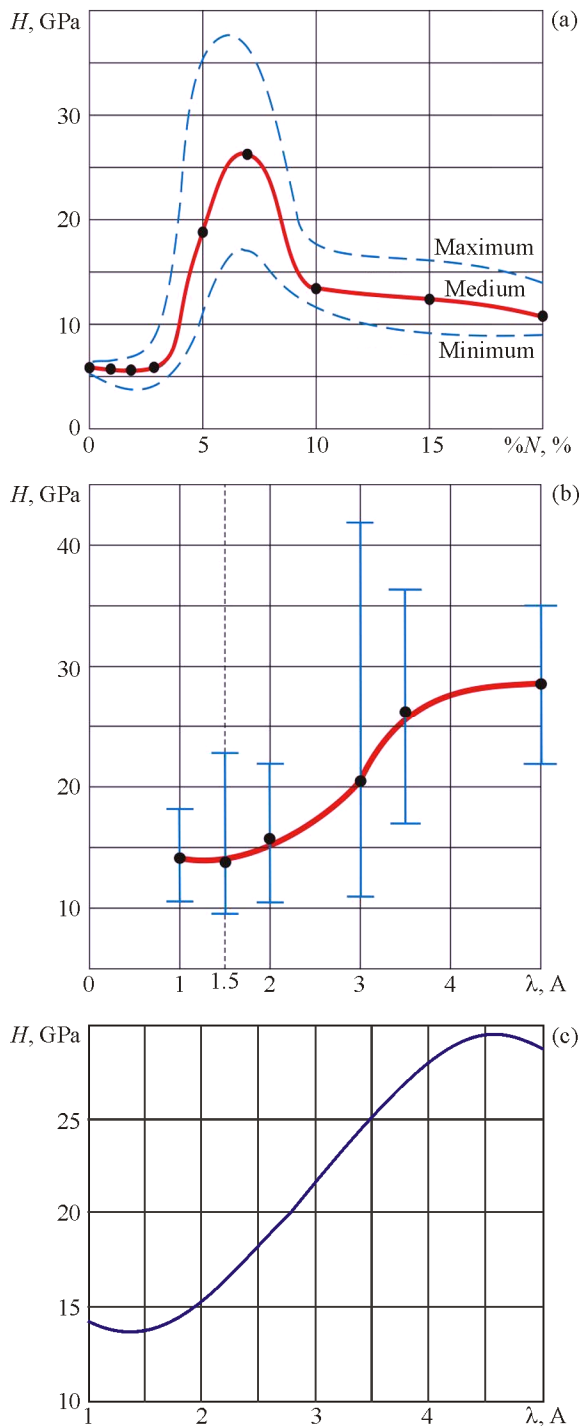


Fig. 5. Experimental curves of hardness H of carbon coatings versus deposition parameters: a—amount of nitrogen in the chamber $\%N$ (% of valve opening), b, c—induction coil current λ : experimental (b) and approximation curve (c) (color online).

Since the induction coil current λ determines the volumetric flux density of deposited carbon ions, the values of λ cannot be too small or too large. At small

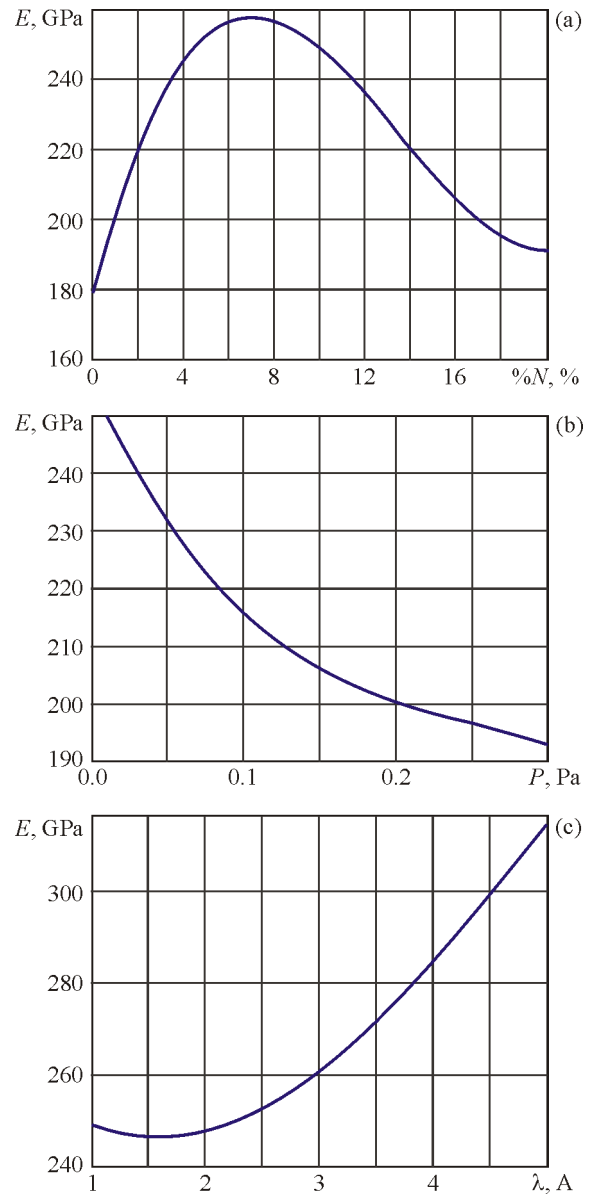


Fig. 6. Approximation curves of elastic modulus E of carbon coatings versus deposition parameters: a—amount of nitrogen in the chamber $\%N$ (% of valve opening), b—chamber pressure P , c—induction coil current λ .

values of λ , the resulting coating is either loose or is deposited too slowly. At large λ , the substrate is ion etched. Therefore, Figs. 5b and 5c show only the range of operating values of λ . This entire range corresponds to a rather high hardness of DLC coatings, and the most optimal values are $\lambda = 3.0\text{--}3.8$ A.

In contrast to the hardness curves, the experimental dependences of elastic modulus E on all three variable parameters $E = f(\%N)$, $E = f(P)$ and $E = f(\lambda)$ are approximated by least squares using a third-degree polynomial with sufficient accuracy ($\text{RMS}_{\%N} =$

19.36 GPa, $RMS_P=0.0933$ GPa, $RMS_\lambda=9.15$ GPa). Therefore, Fig. 6 shows approximated experimental curves plotted using the corresponding polynomial functions (2)–(4):

$$E(\%N) := 179.42 + 25.656\%N - 2.4962\%N^2 + 0.06209\%N^3, \quad (2)$$

$$E(P) := 255.088 - 568.477P + 2027.6312P^2 - 2751.2627P^3, \quad (3)$$

$$E(\lambda) := 268.94 - 30.715\lambda + 11.4374\lambda^2 - 0.69053\lambda^3. \quad (4)$$

The experimental results of Figs. 5 and 6 obtained through data analysis and statistical data processing reveal the following trends:

1) the dependences of H and E on each of the variable parameters $\%N$, P and λ show a completely different behavior,

2) each parameter $\%N$, P and λ changes H and E in a similar way, i.e., the dependences, e.g., $H=f(\%N)$ and $E=f(\%N)$, are almost identical qualitatively.

The first trend indicates that since the three considered variable parameters affect the physical and mechanical properties in different directions, the deposition mode of carbon coatings can and should be optimized with respect to these parameters. The second trend suggests that the effect of the parameters $\%N$, P and λ on the strength properties of coatings (H and E) is not stochastic, but is based on common phenomena and processes whose physical meaning was partially discussed earlier.

Based on the plotted one-parameter curves, it is easy to identify the range of the process parameters $\%N$, P and λ that reliably provide stable physical and mechanical properties of the studied DLC coatings determined by continuous indentation:

– optimal range of variable process parameters: $\%N=5-8$, $\lambda=3.0-3.8$ A,

– predicted physical and mechanical properties of DLC coatings: $H \geq 18-20$ GPa, $E \geq 250$ GPa, $H/E \geq 0.07$, $H^3/E^2 \geq 0.08$ GPa.

The specified level of physical and mechanical characteristics of coatings can be achieved outside the given range of optimal parameter values, but as shown by the analysis of the generated database, stable repeatability of these properties is not guaranteed in this case.

Each of the variable parameters $\%N$, P and λ is considered independent from the point of view of plasma-assisted deposition technology. However, their different effects on H and E indicate the neces-

sity of studying their combined influence. For this purpose, the generated database was used to study the two-parameter (pairwise) effect of the parameters $\%N$, P , λ and t on the hardness H of carbon coatings using machine learning methods and neural network algorithms. Its results are presented in the next section.

3.3. Neural Network Analysis of Database on Carbon Coatings

In addition to classical statistical methods, the results of which are presented in the previous section, we used machine learning algorithms to search for patterns in the experimental database and predict the hardness values of DLC coatings. A criterion for the presence of patterns was the value of the coefficient of determination R^2 .

Let y_i and f_i ($i=1, \dots, n$) be the experimental and predicted values of the unknown function (hardness H), and m be the average value of all y_i , then the value of R^2 is determined as

$$R_{\text{score}}^2 = 1 - \frac{\sum(y_i - f_i)^2}{\sum(y_i - m)^2}. \quad (5)$$

The maximum value of $R^2=1$ corresponds to the best prediction quality. In practice, R^2 can take zero or even negative values if the data is random noise or contains large outliers, as well as for a poorly trained or retrained model.

The first step in constructing machine learning models is to collect data. In this study, a data set for analysis and training included the results of 58 experiments on DLC coating deposition selected from the created database. The input parameters of the models were four experimental parameters: chamber pressure P , the amount of nitrogen supplied to the chamber $\%N$, induction coil current λ , and coating deposition time t . The hardness H of the resulting carbon coating was chosen as the target parameter. The dependence of hardness on experimental parameters was modeled using the linear Ridge algorithm (ridge regression), the ExtraTrees algorithm, which proved to be good for low-dimensional tabular problems [14, 37], and a fully connected multilayer perceptron (MLP) network. Ridge regression is a type of linear regression, also known as Tikhonov regularization. ExtraTrees refers to ensemble algorithms that use decision trees as weak estimators. Due to the relatively small size of the original data set, it was decided to use LeaveOneOut cross-validation approach. Data were normalized before training models.

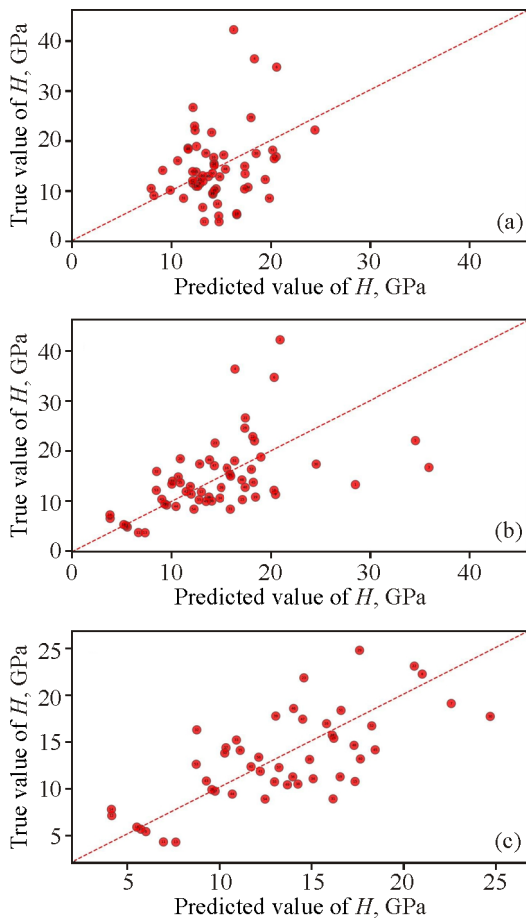


Fig. 7. Scatter plot showing correlations between the experimentally determined true hardness values and the values predicted by the algorithm during cross-validation: a—results for the Ridge regression algorithm, b—for the ExtraTrees ensemble algorithm, c—for the ExtraTrees ensemble algorithm after data filtering (color online).

The predicted hardness value H_{pred} and the experimental value H_{orig} are shown in Fig. 7 for each experiment. Initially, the algorithms were trained on the original data without filtering (Fig. 7). The metric R^2 for unfiltered data was 0.117 for ExtraTrees and 0.045 for Ridge. Both algorithms showed low prediction quality, but most of the points in Fig. 7b are located along the prediction–experiment line, while in Fig. 7a points are scattered randomly. Subsequently, the quality of the model was improved based on an ensemble of trees (ExtraTrees), which revealed a higher correlation in the original experimental data than the Ridge-based model.

It is seen from Fig. 7b that the prediction quality for some experiments is significantly lower. The points with initial ordinal numbers in the database are the most distant from the prediction–experiment line,

i.e., the least predictable hardness values are observed for coatings obtained at the initial stage of testing the modes of plasma-assisted DLC coating deposition. To improve the quality of prediction, we filtered out experiments for which the ExtraTrees algorithm showed the greatest error. The result obtained after data filtering is shown in Fig. 7c. After removing eleven experiments with the largest error, the prediction quality increased significantly up to $R^2=0.45$. The Ridge model was not improved after filtering. The prediction quality of the ExtraTrees algorithm was also improved by selecting parameters such as the maximum tree depth and the total number of trees. The best metric $R^2=0.5$ was obtained by a model with a maximum tree depth of 5 and a total number of trees of 20. The input parameter space has a small dimension of 4 input parameters, which makes it possible to improve the quality of prediction by expanding the feature space. As a result, the quality of prediction was increased to $R^2=0.56$ by adding polynomial features of degree not higher than two, i.e., squares and pairwise products of the original features. The addition of third-degree polynomial features did not lead to further improvement in quality.

The same sequence of improvements as for trees was applied for a fully connected neural network. Initially, the neural network with one hidden layer of 100 neurons, trained on unfiltered data, showed a prediction quality of $R^2<0$. Training the same network on filtered data did not improve the prediction quality. Further, by selecting parameters, as well as the architecture of the neural network, we achieved a prediction quality of $R^2=0$ comparable to the quality of the tree-based model. The corresponding neural network architecture consisted of 2 consecutive hidden layers of 10 neurons each. The L^2 -regularization value during training was equal to 1. Expansion of the feature space did not lead to an increase in the prediction quality of the neural network; the maximum value of R^2 remained equal to 0.5.

Thus, data filtration, feature space expansion and optimization of the algorithm parameters significantly improved the quality of model prediction from $R^2=0.117$ to 0.56 for ExtraTrees and from $R^2<0$ to 0.5 for the neural network. As a result, we obtained models for the dependence of hardness H on experimental parameters, which were used at the next stage of research to visualize the hardness dependences. The results of using the trained ExtraTrees algorithm and neural network to plot the coating hardness variation as a function of pairs of parameters are presented in Fig. 8 in the form of heat color maps. The

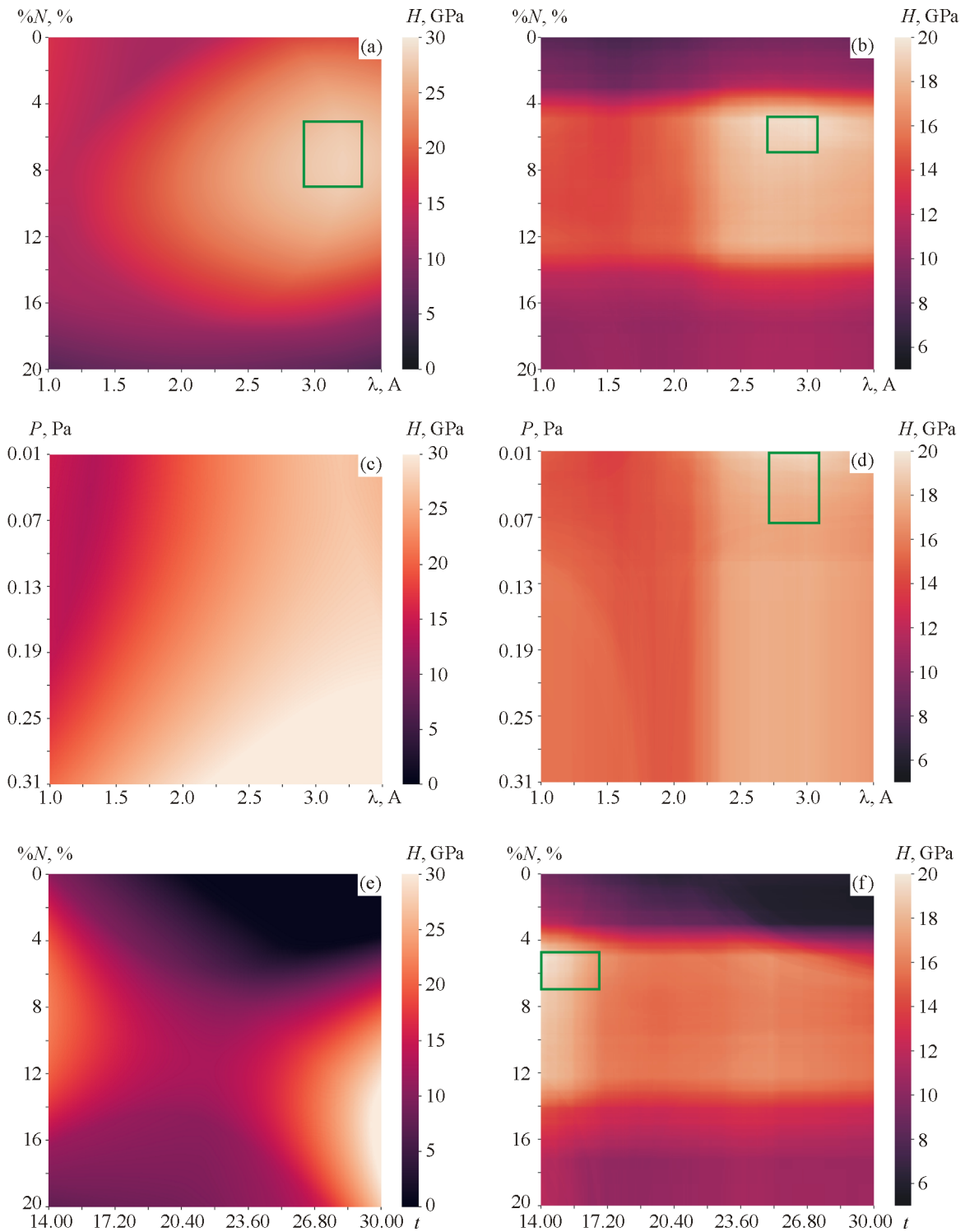


Fig. 8. Two-parameter color maps of hardness plotted using a trained neural network (a, c, e) and a trained ExtraTrees algorithm (b, d, f). Parameter planes: a, b— $\%N-\lambda$, c, d— $P-\lambda$, e, f— $\%N-t$. The hardness color scale in GPa is shown on each map on the right (color online).

prediction of the coating hardness was plotted near the experimental point with the maximum hardness value for all parameter values on the plane. Two-

parameter color maps of hardness were constructed for all possible pairs of input parameters: coil current λ , deposition time t , amount of nitrogen in the flux

Table 3. Optimal parameter values from two-dimensional color maps of DLC coatings (Fig. 8)

Parameters	WorkPress	DeposTime	Npercentage	CoilCurrent
Chamber pressure P , Pa (WorkPress)		<0.02	<0.05	<0.08
Sputtering time t , min (DeposTime)	10–17		10–17	10–17
Nitrogen pressure % N (Npercentage)	5–7	5–7		5–7
Induction coil current λ , A (CoilCurrent)	– 2.7–3.1	0–1.6 2.7–3.1	– 2.7–3.1	

% N , and operating pressure P . Color in Fig. 8 shows the expected value of coating hardness.

In practice, in the technology of plasma-assisted DLC coating deposition, the ranges of permissible values of process parameters for obtaining optimal coating properties turn out to be quite narrow (see Figs. 5 and 6). Comparison of the experimental data from Sect. 3.2 with the numerical analysis data of this section shows more accurate prediction using the ExtraTrees algorithm. Areas of coinciding optimum experimental and predicted parameter values are marked by a rectangular frame in Fig. 8. When predicting with the MLP neural network, it was very problematic to construct such areas for the real values of some pairs of parameters (Figs. 8c and 8e). Data on the optimal input parameter values obtained with the ExtraTrees algorithm and providing the maximum level of coating hardness (Figs. 8b, 8d and 8f) are summarized in Table 3. The optimal values of each parameter are given in the rows of Table 3. The parameter value at the intersection of the row and column in Table 3 corresponds to the two-dimensional color map in Fig. 8.

It is interesting to compare the data in Fig. 5, which are summary results of one-parameter experimental hardness curves from Sect. 3.2, and the data of Table 3, which are summary results of predicted two-parameter dependences from Sect. 3.3. Comparison of these data obtained using different statistical and IT methods shows that the ranges of optimal values of the varied parameters % N , P and λ have a high degree of overlap. Moreover, they are almost identical for the data obtained with the ExtraTrees algorithm. The coincidence of the results obtained by different methods of analyzing the DLC coating database indicates that plasma-assisted deposition technology can be considered as a controlled process, despite its multiparameter, nonequilibrium and stochastic nature.

4. CONCLUSIONS

The use of nitrogen instead of hydrogen for carbon coating stabilization provides stable thickness values of DLC coatings at the level of 0.6–1.4 μm . It also serves as an important process control parameter for adjusting the physical and mechanical characteristics of the deposited coating.

This study showed the possibility to optimize a set of variable DLC coating deposition parameters (chamber pressure P , induction coil current λ , the amount of nitrogen supplied to the chamber % N , deposition time t) in order to enhance the physical and mechanical properties of the coating, such as hardness H and elastic modulus E . The highest accuracy in predicting the carbon coating hardness was achieved through bimodal variation of the parameters % N and λ ; their optimization using various algorithms (e.g., neural network machine learning and ExtraTrees) gave almost identical localization on the parameter plane (Figs. 8a and 8b). It is important that these parameters are independent as they have different physical effects on the coating properties: % N stabilizes the coating structure by reducing internal stresses, and the value of λ determines the flux density of deposited carbon ions. Bimodal variation of other considered parameters did not yield satisfactory optimization results, which were contradictory depending on the algorithms used (Figs. 8e and 8f).

A methodological approach was tested which included the creation of a database of carbon coatings, identification of relationships between deposition parameters and coating properties using statistical data processing, and optimization of the obtained dependences using machine learning algorithms. This approach was shown to solve the problem of stochastic distribution and significant scatter of data caused by the features of an unstable nonequilibrium ion plasma system and a large number of parameters that determine the composition, structure and properties of coatings. As a result, it becomes possible to reliably

predict the coating properties by varying a limited number of process control parameters.

The study showed that despite the large number of parameters, among which there are stochastic parameters, the technology of plasma-assisted physical vapor deposition can be a reliably controlled process. The generated experimental database of DLC coatings allowed us to identify the most significant parameters and determine their effects on the coating properties. The use of machine learning and neural network algorithms expanded the possibilities of using these effects in the form of two-dimensional color maps. The results obtained showed no contradictions when using classical statistical methods and new computer technologies, with the exception of a significant gain in data processing time provided by the latter. Research prospects in the fields of plasma-assisted PVD technologies and unstable nonequilibrium processes with growing database size involve the increasing use of machine learning and neural networks for its analysis instead of conventional statistical processing methods.

FUNDING

The work was carried out with financial support from the Russian Science Foundation (Grant No. 21-79-30007).

CONFLICT OF INTEREST

The authors of this work declare that they have no conflicts of interest.

REFERENCES

1. *Vapor Deposition*, Powell, C.F., Oxley, J.H., and Blocher, J.M., Eds., John Wiley & Sons, 1966.
2. *Handbook of Thin Film Technology*, Maissel, L.I. and Glang, R., Eds., New York: McGraw-Hill, 1970.
3. *Sputtering and Ion Plating: Proc. Conf. on Lewis Research Centre*, Lundin, B.T., Ed., NASA SP-5111, 1972.
4. Vereshchaka, A.S., Tabakov, V.P., and Zhogin, A.S., Carbide Tools with Titanium Nitride Coatings, *Stanki Instrument*, 1976, no. 6, pp. 12–14.
5. Brodyansky, A.P., Tool Hardening on the “Pusk” and “Bulat” Apparatuses, *Tekhnolog. Organizats. Proizvodstv.*, 1977, no. 2, p. 25.
6. Kostzhitsky, A.I. and Lebedinsky, O.V., *Multicomponent Vacuum Coatings*, Moscow: Mashinostroeniye, 1982.
7. Belyi, A.V., Karpenko, G.D., and Myshkin, N.K., *Structure and Production Methods of Wear-Resistant Surface Layers*, Moscow: Mashinostroeniye, 1991.
8. Ilin, A.A., Plikhunov, V.V., Petrov, L.M., and Spektor, V.S., *Plasma-Assisted Vacuum Processing*, Moscow: INFRA-M, 2014.
9. Thornton, A.J., The Influence of Bias Sputter Parameters on Thick Copper Coatings Deposited Using a Hollow Cathode, *Thin Solid Films*, 1977, vol. 40, pp. 335–344. [https://doi.org/10.1016/0040-6090\(77\)90135-3](https://doi.org/10.1016/0040-6090(77)90135-3)
10. Anders, A., A Structure Zone Diagram Including Plasma Based Deposition and Ion Etching, *Thin Solid Films*, 2010, vol. 518, no. 15, pp. 4087–4090. <https://doi.org/10.1016/j.tsf.2009.10.145>
11. Sedlaček, M., Podgornik, B., and Vižintin, J., Tribological Properties of DLC Coatings and Comparison with Test Results: Development of a Database, *Mater. Character.*, 2008, vol. 59, no. 2, pp. 151–161. <https://doi.org/10.1016/j.matchar.2006.12.008>
12. MacLeod, B.P., Self-Driving Laboratory for Accelerated Discovery of Thin-Film Materials, *Sci. Adv.*, 2020, vol. 6, no. 20, p. eaaz8867. <https://doi.org/10.1126/sciadv.aaz8867>
13. Ohkubo, I., Realization of Closed-Loop Optimization of Epitaxial Titanium Nitride Thin-Film Growth Via Machine Learning, *Mater. Today Phys.*, 2021, vol. 16, p. 100296. <https://doi.org/10.1016/j.mtphys.2020.100296>
14. Lifar, M.S., Guda, S.A., Kudryakov, O.V., Guda, A.A., Pashkov, D.M., Rusalev, Yu.V., Migal, Yu.F., Soldatov, A.V., and Kolesnikov, V.I., Relationships between Synthesis Conditions and TiN Coating Properties Discovered from the Data Driven Approach, *Thin Solid Films*, 2023, vol. 768, p. 139725. <https://doi.org/10.1016/j.tsf.2023.139725>
15. Ershov, I.V., Prutsakova, N.V., Kholodova, O.M., Lavrentyev, A.A., Mardasova, I.V., and Zhdanova, T.P., Structural Properties and Composition of Graphite-Like Carbon Films Obtained by Pulsed Laser Deposition, *Tech. Phys.*, 2021, vol. 66, pp. 580–587. <https://doi.org/10.1134/S1063784221040071>
16. Bleu, Y., Bourquard, F., Tite, T., Loir, A.-S., Madidi, Ch., Donnet, C., and Garrelie, F., Review of Graphene Growth from a Solid Carbon Source by Pulsed Laser Deposition (PLD), *Front. Chem.*, 2018, vol. 6 (Systematic Review). <https://doi.org/10.3389/fchem.2018.00572>
17. Kolesnikov, V.I., Vereskun, V.D., Kudryakov, O.V., Manturov, D.S., Popov, O.N., and Novikov, E.S., Technologies for Improving the Wear Resistance of Heavily Loaded Tribosystems and Their Monitoring. *J. Frict. Wear*, 2020, vol. 41, pp. 169–173. <https://doi.org/10.3103/S1068366620020051>
18. Kolesnikov, V.I., Kudryakov, O.V., Zabiya, I.Yu., Novikov, E.S., and Manturov, D.S., Structural Aspects of Wear Resistance of Coatings Deposited by Physical Vapor Deposition, *Phys. Mesomech.*, 2020, vol. 23, no. 6, pp. 570–583. <https://doi.org/10.1134/S1029959920060132>
19. Kudryakov, O.V., Varavka, V.N., Kolesnikov, I.V., Novikov, E.S., and Zabiya, I.Yu., DLC Coatings for

- Tribotechnical Purposes: Features of the Structure and Wear Resistance, *IOP Conf. Mater. Sci. Eng.*, 2021, vol. 1029, no. 1, p. 012061. <https://doi.org/10.1088/1757-899X/1029/1/012061>
20. Charitidis, C.A., Nanomechanical and Nanotribological Properties of Carbon-Based Thin Films: A Review, *Int. J. Refract. Met. Hard Mater.*, 2010, vol. 28, p. 51. <https://doi.org/10.1016/j.ijrmhm.2009.08.003>
 21. Charitidis, C.A., Koumoulos, E.P., and Dragatogianis, D.A., Nanotribological Behavior of Carbon Based Thin Films: Friction and Lubricity Mechanisms at the Nanoscale, *Lubricants*, 2013, vol. 1, pp. 22–47. <https://doi.org/10.3390/lubricants1020022>
 22. Riedo, E., Chevrier, J., Comin, F., and Brune, H., Nanotribology of Carbon-Based Thin Films: The Influence of Film Structure and Surface Morphology, *Surf. Sci.*, 2001, vol. 477, p. 25.
 23. Golovin, Yu.I., *Nanoindentation and Its Capabilities*, Moscow: Mashinostroeniye, 2009.
 24. *GOST 8.748-2011 (ISO 14577-1:2002): Metallic Materials. Instrumented Indentation Test for Hardness and Materials Parameters. Part 1: Test Method.*
 25. *GOST R 50779.25-2005 (ISO 3494:1976): Statistical Methods. Statistical Interpretation of Data. Power of Tests Relating to Means and Variances.*
 26. *GOST R ISO 16269-4-2017: Statistical Methods. Statistical Data Presentation. Part 4: Detection and Treatment of Outliers.*
 27. Rebholz, C., Ziegele, H., Leyland, A., and Matthews, A., Structure, Mechanical and Tribological Properties of Nitrogen-Containing Chromium Coatings Prepared by Reactive Magnetron Sputtering, *Surf. Coat. Technol.*, 1999, vol. 115, pp. 222–229. [https://doi.org/10.1016/S0257-8972\(99\)00240-6](https://doi.org/10.1016/S0257-8972(99)00240-6)
 28. *Nanostructured Coatings*, Cavaleiro, A. and Hosson, J.Th.M., Eds., New York: Springer, 2006.
 29. Pogrebnyak, A.D., Lozovan, A.A., Kirik, G.V., Shchitov, N.N., Stadnik, A.D., and Bratushka, S.N., *Structure and Properties of Nanocomposite, Hybrid and Polymer Coatings*, Moscow: LIBROKOM, 2011.
 30. Kudryakov, O.V., Varavka, V.N., and Kolesnikov, I.V., Self-Healing of PVD-Coatings, *Mater. Sci. Forum*, 2022, vol. 1052, pp. 44–49. <https://doi.org/10.4028/p-996e4s>
 31. Kovaleva, M.G., Kolpakov, A.Ya., Poplavsky, A.I., Galkina, M.E., Gerus, Zh.V., Lyubushkin, R.A., and Mishunin, M.V., Properties of Coatings Based on Carbon and Nitrogen-Doped Carbon Obtained Using a Pulsed Vacuum Arc Method, *J. Frict. Wear*, 2018, vol. 39, pp. 345–348. <https://doi.org/10.3103/S1068366618040074>
 32. Baba, K., Hatada, R., Flege, S., and Ensinger, W., Diamond-Like Carbon Films with Low Internal Stress by a Simple Bilayer Approach, *Coatings*, 2020, vol. 10(7), p. 696. <https://doi.org/10.3390/coatings10070696>
 33. Haas, T.W., Grant, J.T., and Dooley, G.J., Chemical Effects in Auger Electron Spectroscopy, *J. Appl. Phys.*, 1972, vol. 43, pp. 1853–1860. <https://doi.org/10.1063/1.1661409>
 34. Lurie, P.G. and Wilson, J.M., The Diamond Surface: Secondary Electron Emission, *Surf. Sci.*, 1977, vol. 65, no. 2, pp. 476–498. [https://doi.org/10.1016/0039-6028\(77\)90460-5](https://doi.org/10.1016/0039-6028(77)90460-5)
 35. Sidashov, A.V., *Electronic Structure, Elemental Composition and Strength Properties of Laser-Modified Surfaces of Steel and Diamond and Graphene Films for Tribological Applications*, Doct. Degree Thesis (Phys. & Math.), Rostov-on-Don: YuFU, 2022.
 36. Dementjev, A.P. and Petukhov, M.N., Comparison of X-Ray-Excited Auger Lineshapes of Graphite, Polyethylene and Diamond, *Surf. Interface Analysis*, 1996, vol. 24, pp. 517–521. [https://doi.org/10.1002/\(SICI\)1096-9918\(199608\)24:8<517::AID-SIA154>3.0.CO;2-L](https://doi.org/10.1002/(SICI)1096-9918(199608)24:8<517::AID-SIA154>3.0.CO;2-L)
 37. Geurts, P., Ernst, D., and Wehenkel, L., Extremely Randomized Trees, *Machine Learning*, 2006, vol. 63, no. 1, pp. 3–42. <https://doi.org/10.1007/s10994-006-6226-1>

Publisher's Note. Pleiades Publishing remains neutral with regard to jurisdictional claims in published maps and institutional affiliations.